Research paper

A novel cooperative compensation method to compensate for return stroke of stick-slip piezoelectric actuators

Cancheng Qiu [a], Jie Ling [a,*], Yangkun Zhang [b], Min Ming [a], Zhao Feng [a], Xiaohui Xiao [a]

[a] School of Power and Mechanical Engineering, Wuhan University, Wuhan 430072, China
[b] Harbin Institute of Technology Shenzhen Graduate School, Shenzhen 518000, China

A R T I C L E   I N F O

A B S T R A C T

With the development of micro-electromechanical systems, high precision actuators with high resolution, fast speed, large load capacity are increasingly required. Thanks to the characteristics of flexible structure, fast step speed, low energy consumption, high resolution and unlimited stroke range, stick-slip actuators have been drawing worldwide attention. Traditionally, stick-slip actuators are driven by sawtooth waveform signals with a slow increase and a fast decrease. Therefore, there is an unavoidable return stroke when fast decrease of the driving signal appears, which reduces driving speed and efficiency. In this paper, a novel cooperative compensation method (CCM) to compensate for return stroke of stick-slip actuators is proposed. It uses two signals of specific initial time gap (ITG) to reduce the return stroke to improve speed. A modified two-layer stick-slip piezoelectric actuator based on a triangular compliant driving mechanism is built. Experimental results show that the CCM can effectively increase step size of the actuator, especially driven under low frequencies. When signal is at 10 Hz, the step size of the actuator With CCM is over 29 times of that with traditional single-PSA-driving method (TSM). The maximum step size with CCM is 4.448 μm at 250 Hz, which is more than 40% of TSM.

1. Introduction

High precision actuators, as the core element in high precision positioning systems [1], play vital roles in many scientific and industrial fields, such as biomedicine [2,3], optical systems [4,5], micro-machinery [6], micro-manipulation [7,8], aerospace [9], fiber-optic communication [10], etc. Piezoelectric materials, which can achieve nanometer level resolution and generate high output force up to thousands of Newtons, is an ideal material for high precision driving, having drawn widespread attention. Therefore, various types of piezoelectric actuators, including stick-slip type [12–14,11], inchworm type [15–17], direct-push type [18], ultrasonic type [19,20], and hybrid type [21], have been rapidly developed in recent years. Among them, stick-slip actuators attract special interest due to their edge in flexible structure, simple controlling, fast step speed, high resolution and unlimited stroke range.

---

* Corresponding author.
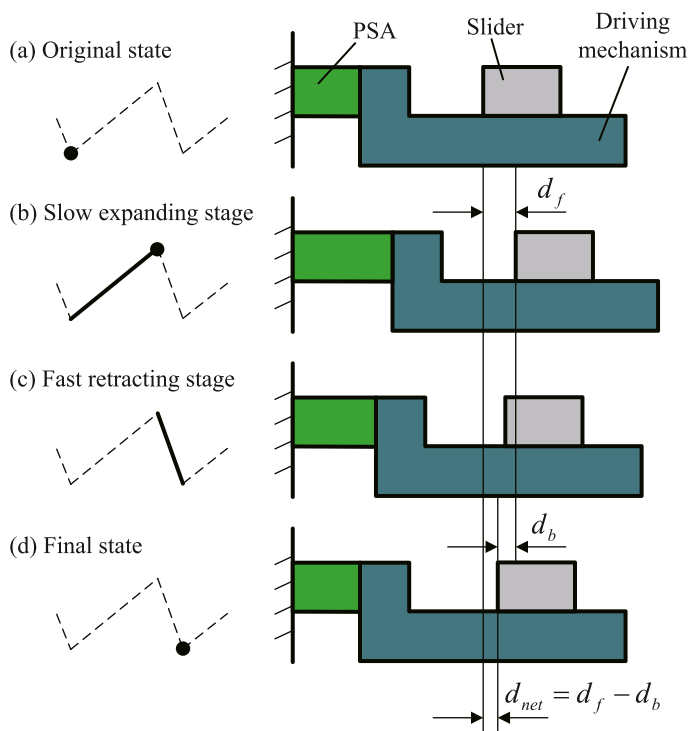*E-mail address:* jamesling@whu.edu.cn (J. Ling).

Fig. 1. Configuration and operating principle of a typical stick-slip actuator.

As shown in Fig. 1, a typical stick-slip actuator is mainly consisted of a piezoelectric stack actuator (PSA), a driving mechanism, and a slider (or end-effector). The driving foot is the part of driving mechanism contacting to slider. The slider is driving by friction force produced in the relative motion between driving foot and slider. A sawtooth waveform signal of a slow increase and a fast decrease is applied to the PSA. The motion process contains two stages: slow expansion stage and fast contraction stage. In the slow expansion stage, or the "stick" stage, the compliant mechanism is driving by PSA to push slider forward with no relative motion. In the fast contraction stage, or the "slip" stage, the compliant mechanism returns to its origin condition rapidly. There is relative motion between driving foot and slider. Apparently, return stroke d_b of the slider is smaller than forward stroke d_f, so in each period there is a net forward displacement d_{net} of the slider. One period after another, the slider moves forward as d_{net} accumulates.

Speed of end-effector is a main index when a stick-slip actuator is being evaluated [22]. Speed can be improved directly by increasing voltage amplitude or frequency of sawtooth waveform signal. The sawtooth waveform voltage signal applied to PSA is produced by function generator and is amplified by voltage amplifier. Since the maximum allowable voltage is limited, increasing frequency of signal is an efficient option chosen by many researchers to raise the speed of stick-slip actuators [13,14]. However, frequency of the voltage signal is generally limited by bandwidth of the actuator [23] and maximum allowable frequency of PSAs, which means PSA and voltage amplifier of extremely high performance are required. Besides, spectrum of sawtooth waveform signal contains sine signals of base frequency f and its multiples based on Fourier transform. Therefore, it requires driving mechanism with high bandwidth. high-order harmonics of the signal is greatly likely to be attenuated. Other researchers come up with modified sawtooth waveform voltage signal to improve speed performance, either by adopting a cycloid decrease instead of a direct decrease [14] or adding time delays of specific lengths before and after fast contraction stage [24]. Recently, a novel sequential control method (SCM) is used to suppress the backward motion of stick-slip actuator [25]. A two-layer structure composed of driving part and lifting part. When PSA of driving part contracts, PSA of lifting part expand to stop the slider from moving back. Backward motion is perfectly suppressed but there is always a plateau in each period.

Aiming to increase the speed of end-effector, a cooperative compensation method (CCM) to compensate for return stroke of stick-slip actuators is proposed in the paper. Traditionally, piezoelectric stick-slip actuator is driven by a single PSA in a direction [26–28]. An established stick-slip piezoelectric actuator based on a triangular compliant driving mechanism [13] is modified into a two-layer structure. Two layers of the mechanism are used to drive the slider in one direction sequentially to compensate the return stroke. With a smaller return stroke d_b, a larger net forward displacement d_{net} is obtained, and then a faster speed and better driving efficiency are obtained. Therefore, compared with traditional single-PSA-driving method (TSM), the superiority of the proposed driving method is two-fold: (1) Smaller return stroke for improved driving efficiency;
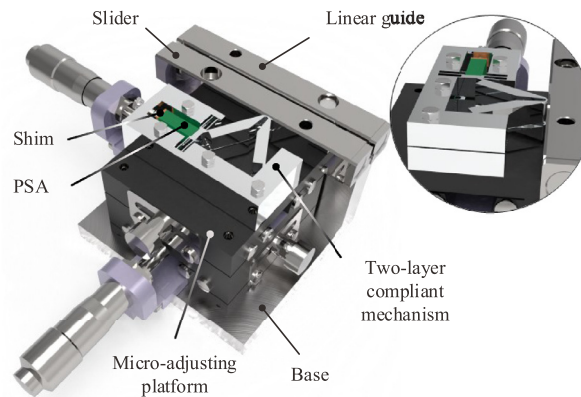
Fig. 2. Three-dimensional model of the proposed piezoelectric stick-slip actuator.
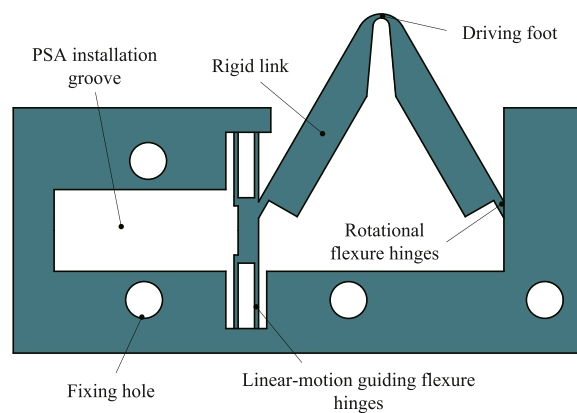

Fig. 3. Structural model of modified triangular compliant mechanism proposed in [13].

(2) Reduced requirements for voltage amplifiers with accelerated speed even under a lower driving frequency. Otherwise, the TSM with single signal is preserved, and it can switch between these two methods according to actual needs.

The rest of paper is divided into four sections. The configuration and the operating principle of the stick-slip actuator with compensation of return stroke is introduced in Section 2. In Section 3, the compliant driving mechanism is analyzed kinematically. In Section 4, experiment system is established and a series experiments are conducted to validate the effectiveness of the proposed driving strategy and finally the paper is concluded in Section 5.

2. Configuration and operating principle

In this section, an existing piezoelectric stick-slip actuator based on a triangular compliant driving mechanism modified into a two-layer structure is introduced and used as an example to explain the CCM for return stroke. Configuration of the actuator and operating principle of the driving strategy for compensation for return stroke is illustrated as following.

2.1. Configuration

The three-dimensional model of the stick-slip actuator, shown in Fig. 2, is composed of a two-layer triangular compliant mechanism, two PSAs, shims, a base, a linear guider, a slider, a micro-adjusting platform, etc. The base is fixed on vibration isolation table with screws. Linear guider and micro-adjusting platform are mounted on the base. Micro-adjusting platform, on which compliant mechanism is installed, is used for control of preload between driving foot and the slider. The structural model of the triangular compliant mechanisms as shown in Fig. 3, which is firstly proposed in [13], is consisted of driving foot, rotational flexure hinges, rigid links, PSA installation notches, fixing holes, etc. It should be noted that, in this work, we used the reported mechanism in [13] to build a two-layer structure and then to validate the effectiveness of the proposed driving method. Without loss of generality, the mechanism for each layer can be replaced by any other stick-slip actuator as proposed in [14,17,26,28–32].
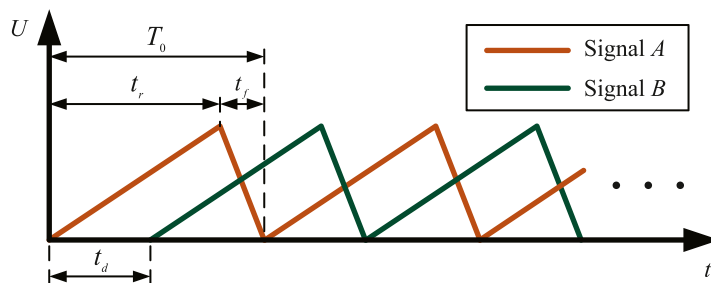
Fig. 4. Sawtooth waveform voltage signals applied to PSAs *A* and *B* in CCM.
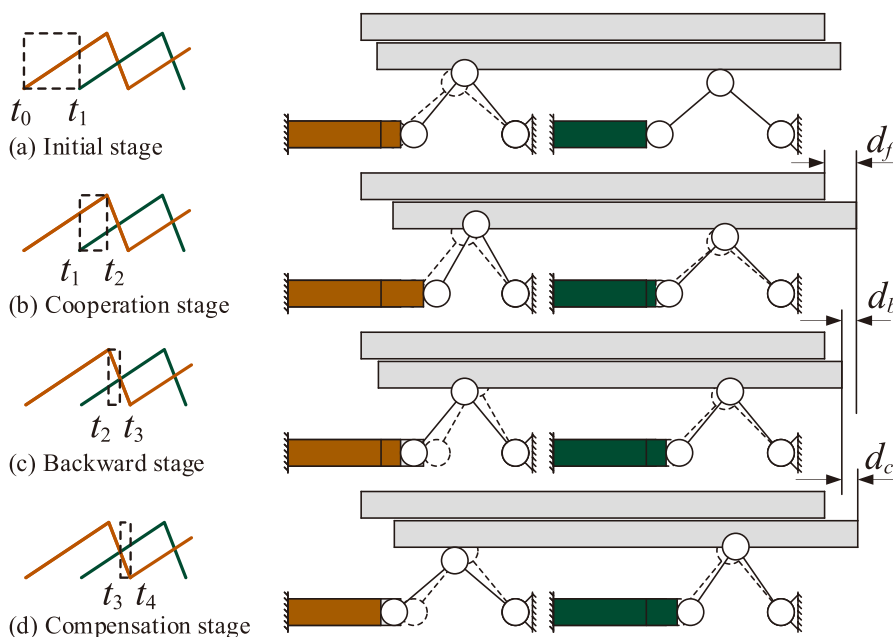

Fig. 5. Operating principle of the proposed CCM for return stroke of stick-slip actuators.

2.2. Operating principle

In the proposed CCM, there are two signals compensating each other used to control one-directional motion of slip-slip actuator. The sawtooth waveform voltage signals, shown in Fig. 4, are applied to PSAs *A* and *B*, respectively. Period of both signals is T, divided into rise time t_r and fall time t_f. t_d denotes the ITG of two signals.

As Fig. 5 shows, the working process is divided into four stages: initial stage, cooperative stage, backward stage and compensation stage. In order to show the process explicitly, the two-layer structure is shown as two separate parts.

(1) Initial stage From t_0 to t_1, PSA *A* expands first as signal *A* increases slowly while PSA *B* stand still with no voltage applied. The slider moves forward. It should be pointed out that the initial stage only appears once at the very beginning of a complete driving process.

(2) Cooperative stage From t_1 to t_2, PSA *B* begins to expand with the same speed of PSA *A*. In this stage, PSA *A* plays a leading role. The slider moves forward by the static friction between driving foot and itself. The forward displacement is noted as d_f.

(3) Backward stage The stage begins when PSA *A* reaches to its maximum length and is about to fall. In the stage, PSA *B* continues to expand, but the length of it is smaller than PSA *A*'s. The slider follows PSA *A* to move backward, the backward displacement of which is notes as d_b.

(4) Compensation stage PSA *B* continues to expand while PSA *A* is contracting fast, which suppress backward motion of the slider following PSA *A*. In this stage, PSA *B* plays a leading role in driving the slider. The compensation displacement is noted as d_c.
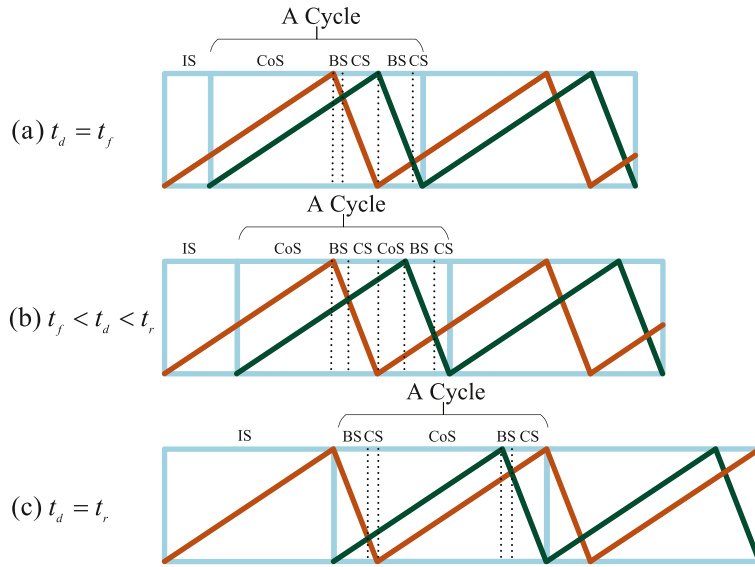
Fig. 6. Operating processes of different ITG. (IS = Initial Stage, CoS = Cooperative Stage, BS = Backward Stage, CS = Compensation Stage).
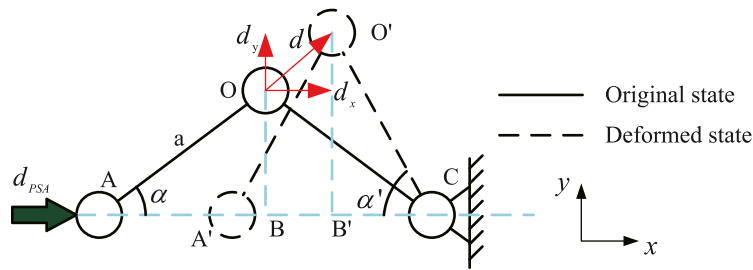

Fig. 7. Kinematics model of the modified triangular compliant mechanism.

As the process moves in cycles, when one PSA is in contraction, another one continues to expand to compensate. The actual period of a cycle remains T_0. The net displacement of a period, or called step size, is calculated as follow:

$$d_{net} = d_f - d_b + d_c \tag{1}$$

To make the process go forward as sequences above, the range of ITG is restricted as follows:

$$\begin{cases} t_d \leqslant t_r \\ t_d + t_r \geqslant T \end{cases} \Rightarrow t_f \leqslant t_d \leqslant t_r \tag{2}$$

Additionally, it is worth noticing that duration and arrangement of these stages are different with unequal ITGs, shown in Fig. 6. In each period, the backward stage and the compensation stage always appear in pairs, and durations of each stage with different ITG are same.

3. Design and analysis

In this section, the modified two-layer triangular compliant mechanism is analyzed kinematically with Pseudo-rigid-body model to determine the structural parameters of the mechanism.

As shown in Fig. 7, pseudo-rigid-body model of the modified compliant mechanism is built to obtain the output characteristics of the mechanism. Applied with given signal, the PSA expands along x direction, and output displacement of the PSA is noted as d_{PSA}. The rotational flexure hinges in mechanism is driven to deform in both x and y directions from original state into deformed state, shown in Fig. 7. The driving foot displacement d is decomposed into d_x along x direction and d_y along y direction. According to geometry relations, following equations can be obtained:

$$a \sin \alpha' = a \sin \alpha + d_y \tag{3}$$

$$a \cos \alpha' = a \cos \alpha - d_x \tag{4}$$

Table 1

Design parameters of modified triangular compliant mechanism.

Parameters	Value	Parameters	Value
a	27 mm	d_x	5 μm
α	60°	d_y	2.886 μm
d_{PSA}	10 mm	R	0.5572

$$2a\cos\alpha = 2a\cos\alpha' + d_{PSA} \tag{5}$$

where a denotes the length of rigid link OA (or OC); α is original angle between OA and x direction; α' is the angle of OA' (or O'C) and x direction, in which OA' is the deformed state of OA.

Relation of d_x and d_{PSA} is calculated with Eq. (4) and (5).

$$d_{PSA} = 2d_x \tag{6}$$

From Eq. (6), output displacement of driving foot is solely related to input displacement of PSA. The amplify ratio is 0.5. By adding squares of Eq. (3) and (4), variable α' can be eliminated.

$$d_y^2 + 2a\sin\alpha \cdot d_y + d_x^2 - 2d_x a\cos\alpha = 0 \tag{7}$$

With Eq. (7), expression of d_y can be achieved.

$$d_y = -a\sin\alpha + \sqrt{a^2(\sin\alpha)^2 + 2\,d_x a\cos\alpha - d_x^2} \tag{8}$$

Therefore, the ratio R of d_y and d_x is calculated according to Eq. (5) and (8).

$$R = \frac{d_y}{d_x} = \frac{-2a\sin\alpha + \sqrt{4a^2(\sin\alpha)^2 + 4\,d_{PSA}a\cos\alpha - d_{PSA}^2}}{d_{PSA}} \tag{9}$$

From Eq. (9), we can conclude that there are three parameters, a, α and d_{PSA}, that determine output characteristics of the compliant mechanism. a and α are structural parameters of the compliant mechanism, and they are unchangeable once designed and fabricated. In practical operation, d_{PSA} is the only parameter that can be used to adjust the output displacement of the slider. d_{PSA} is determined by the amplitude of voltage signal applied to PSA.

Actually, the output displacement is extremely small compared to structural parameters, thus the difference of angle α' and α can be ignored. Therefore, simplified expression can be obtained as follows:

$$d_y' = d_x\cot\alpha \tag{10}$$

$$R' = \frac{d_y'}{d_x} = \cot\alpha \tag{11}$$

Input displacement of PSA is set as 10 μm. A smaller R means that output displacement is mainly used for driving, so driving efficiency can be improved with a proper value of R. Design parameters and theoretical output displacement of slider are shown in Table 1 according to analyses above.
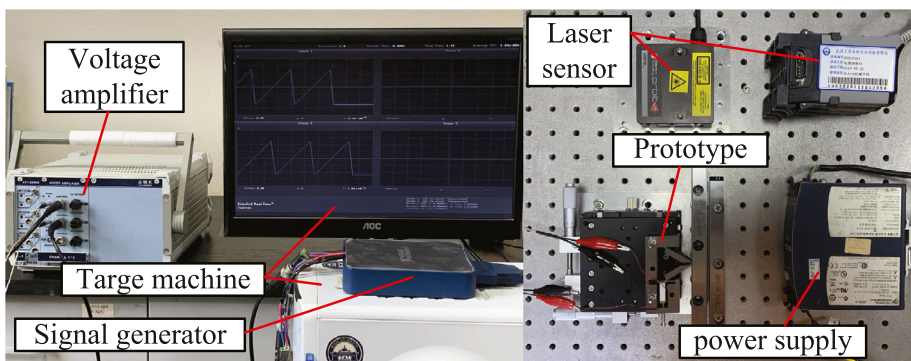
4. Experiments

In this section, a prototype of the modified two-layer stick-slip actuator is fabricated for a series of experiments to investigate driving characteristics and validate the superiority of the CCM in increasing step size and speed.

4.1. Experimental set-up

Experiment system was established as shown in Fig. 8a with the schematic diagram shown in Fig. 8b. Target machine is connected to host computer via Simulink Real-Time. A signal generator (PCI-6289 from National Instruments) is connected to the target machine to generate required sawtooth waveform signals. Signals are amplified by voltage amplifier (E09.S3 from Harbin Core Tomorrow Science & Technology Co., Ltd.) to drive PSAs (PSt 150/55/20H from Harbin Core Tomorrow Science & Technology Co., Ltd.). A laser displacement sensor (Orbit LTH form Ametek Solartron Metrology) is used to measure the output displacement of the slider.

The two-layer triangular compliant mechanism is processed by wire-cut electrical discharge machining. The size of PSA (PSt 150/5 × 5/20H from Harbin Core Tomorrow Science & Technology Co., Ltd.) is 5 mm × 5 mm × 18 mm, and its range is 20 μm. Cross roller guide (VR6-150H10Z from THK Co., Ltd.) is selected as linear guide and slider to provide rigid yet supple linear motion.

(a)
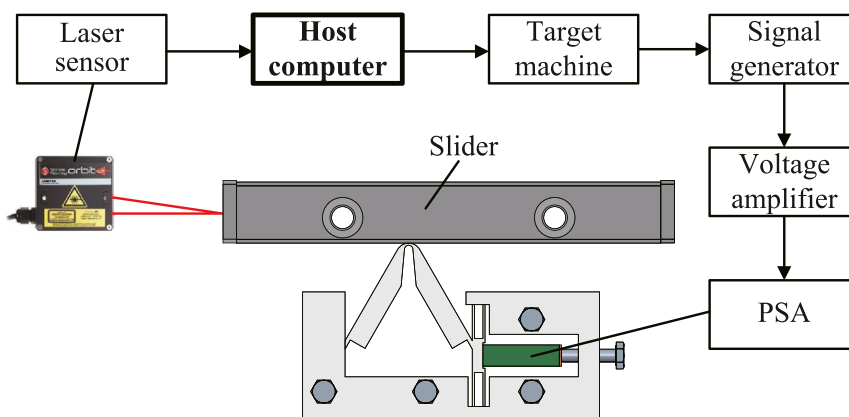
(b)

Fig. 8. Experiment system. (a) Experiment setup; (b) Schematic diagram.

4.2. Experiments and discussion

In order to figure out driving performance of the CCM for return stroke of stick-slip actuator, a series of experiments are carried out. Ratio of rise time t_r and fall time t_f of signals applied are set as 9:1, which means d_f is T/10 and t_r is 9T/10. In experiments, signals of different ITGs and frequencies are applied to the PSAs, and corresponding input displacement are exerted onto compliant mechanism.

ITG is the first parameter of sawtooth waveform signals in CCM to take into consideration. In a series of experiments, signals of different ITGs are applied to the modified two-layer compliant mechanism to find out the best ITG for driving. Frequency is fixed at 200 Hz. According to Eq. (2), the range of t_d is from T/10 to 9T/10. Output displacement of the slider is shown in Fig. 9. It proves that the step size and speed of slider improve greatly with ITG applied. From the figure, it can be concluded that the one with ITG of T/4 shows the best speed performance when frequency is fixed at 200 Hz. Additionally, Fig. 10 shows the output displacement and step size error of the slider at 200 Hz with the ITG of T/4. The average step size is calculated as 4.066 µm, and the standard deviation is 0.1717, which shows the stability and repeatability of the CCM.

Furthermore, a few groups of experiments of different frequencies are carried out to understand whether ITG of T/4 still performs best in cases of different frequencies. Experimental results are organized in Fig. 11. Table 2 shows the comparison of step size and speed between TSM and CCM of best performance. Unfortunately, results show that ITG of T/4 does not always performs best in every cases. Therefore, it should be noted that optimal value of ITG is not fixed in any cases. For different driving mechanisms, driving signals or driving frequencies, optimal value of ITG can be obtained by a series of experiment under the same conditions. It is worth noticing that the CCM is also applicable for other mechanisms besides triangular mechanism, such as Z-shaped actuator [29], parallelogram-type actuator [30], shared-foot-type actuator [31], trapezoid-type actuator [32], etc. It can also increase their speed and reduce the requirement of high frequency.

Table 2
Step size and velocity of slider driven by TSM and CCM of best performance.

Frequency of signal (Hz)	ITG	d_{net} (μm)	v (μm/s)
10	0	0.033	0.334
	T/4	0.97	9.700
50	0	0.133	6.630
	T/4	1.826	91.304
100	0	0.303	30.253
	9T/10	3.366	336.626
150	0	0.402	60.352
	T/2	3.461	519.188
200	0	1.774	354.704
	T/4	4.066	813.202
250	0	3.171	792.828
	T/4	4.448	1111.939
300	0	2.737	820.971
	3T/4	3.876	1162.936
400	0	2.287	914.761
	T/2	3.553	1421.269
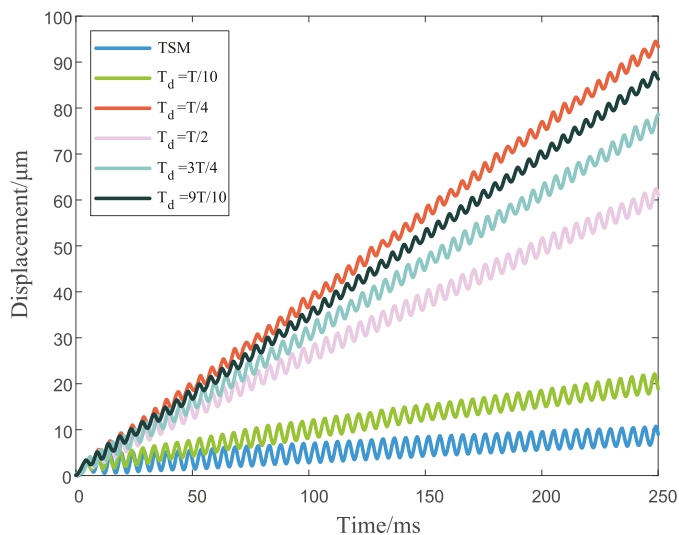
Fig. 9. Output displacement of the slider with different ITGs at 200 Hz.
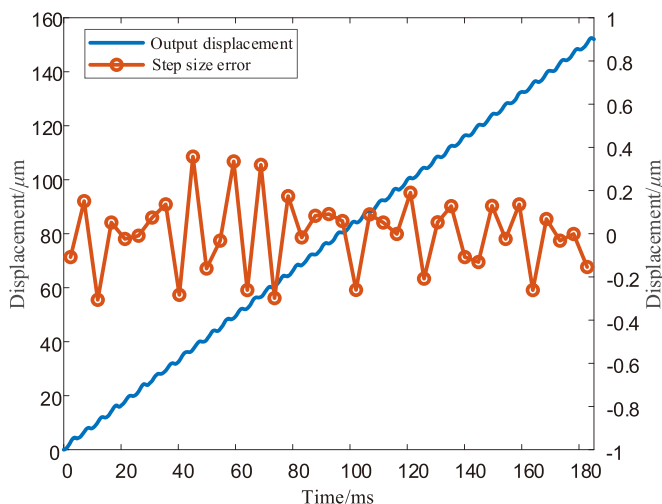
Fig. 10. Output displacement and step size error of the slider at 200 Hz with the ITG of T/4.
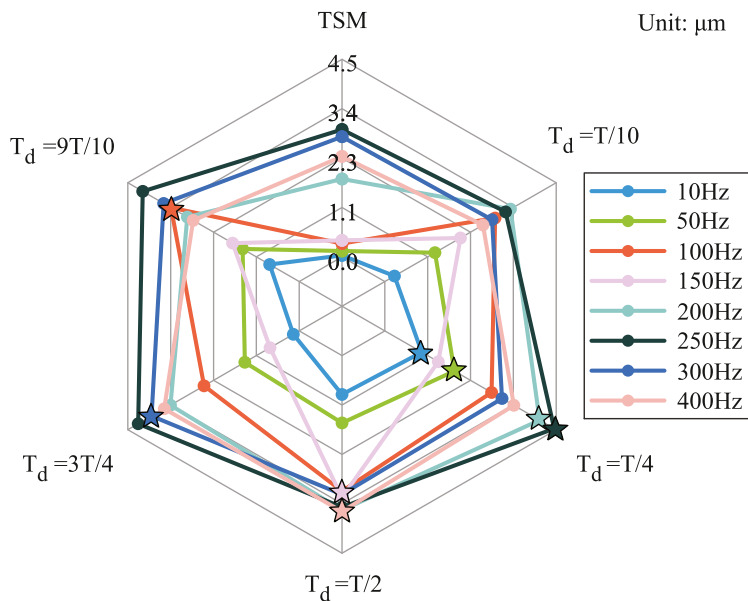
Fig. 11. Experimental results of step size with TSM and CCM. The ☆ mark means the CCM of best performance.
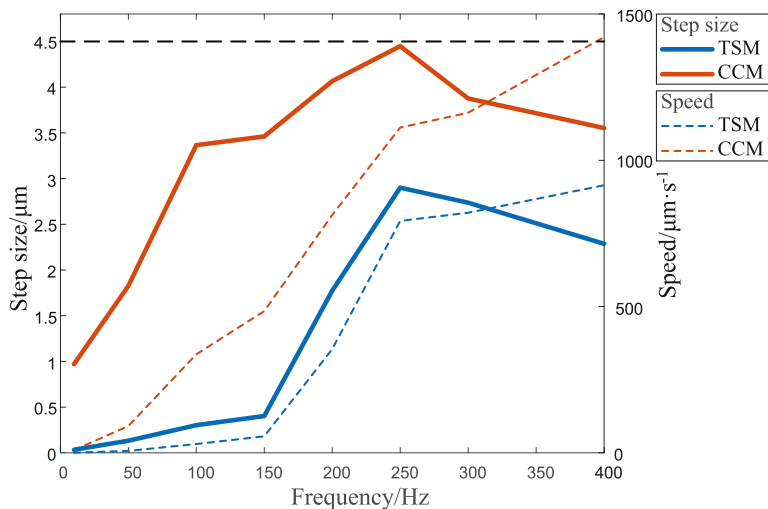

Fig. 12. Step size and speed of the slider with CCM and TSM.

For piezoelectric actuators, step size is an essential optimization goal. In following experiments, relation between step size and frequency of driving signals are investigated. According to Eq. (6), step size in definitely less than $d_{PSA}/2$ in TSM. In our experiments, voltage amplitude of signals applied to PSAs is fixed at 75 V, and corresponding d_{PSA} is tested to be 9 μm. Therefore, the ideal maximum step size can be achieved is 4.5 μm in TSM, which is actually almost unattainable. As shown in Fig. 12, step size and speed of CCM is apparently larger than TSM. At the frequency of 250 Hz, the step size is remarkably close to 4.5 μm, which means that the return stoke is almost eliminated in CCM. Step size peaks at 250 Hz and then declines due to the limited bandwidth of voltage amplifier and the actuator. Since $v = f \cdot d_{net}$, the proposed CCM increases step size by compensating for return stroke to increase speed of the slider.

As shown in Fig. 13, Step size amplification ratio, which is defined as the ratio of step size in CCM and TSM, performs great especially under lower frequencies. The output step size and speed of the slider are hardly affected by limited bandwidth of driving mechanism when driven by low frequency signals. Therefore, increment of step size at low frequencies can better demonstrate advantages of the CCM. When frequency of driving signals is 10 Hz, as shown in Table 2, the step size driven with CCM is 0.97 μm, which is over 20 times of the one with TSM. The significant improvement of step size,
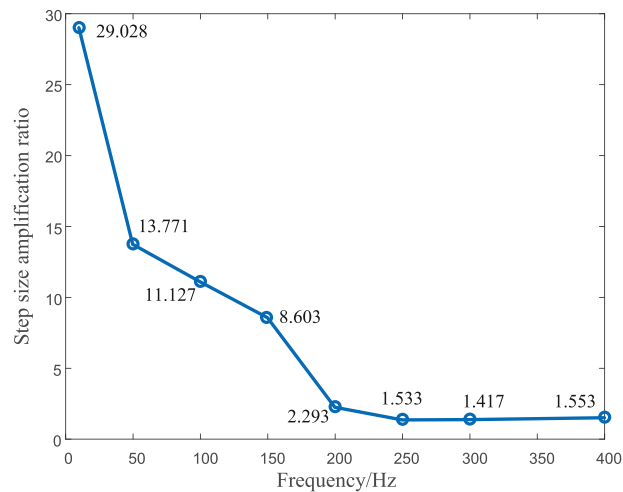
Fig. 13. Step size amplification ratio of CCM and TSM.

especially under low frequencies, illustrates explicitly the superiority of the CCM, ruled out the influence of structure of the mechanism, which means the CCM have a pervasive usability to any other stick-slip actuators based on similar compliant mechanisms.

5. Conclusion

In this work, a novel driving strategy for compensation of return stroke, called CCM, for stick-slip piezoelectric actuators based on a two-layer compliant triangular mechanism is proposed and experimentally validated.

Compared with TSM, a compensation stage is added to working process of the CCM, which increases step size in a cycle to improve driving speed and efficiency. Kinematics analysis of the modified two-layer compliant mechanism was conducted. A two-layer prototype was built, and experiment system was established. A series of experiments were carried out. The superiority of improved driving efficiency and reduced bandwidth requirements for voltage amplifier is validated. The step size obtained with the proposed CCM is improved a lot compared to that with the TSM. Hence, the proposed driving method is more practical as the requirements of the voltage amplifier can be obviously reduced. Under the driving signal at 250 Hz, the return stroke is almost eliminated. Under the driving frequency of 10 Hz, step size of CCM is over 29 times of TSM.

In future work, further investigations on the feed forward controller combined with the CCM for stick-slip actuators are required for better stability and repeatability. Precision controlling of lag time of two voltage amplifiers is supposed to be studied.

Declaration of Competing Interest

The authors declare that they have no known competing financial interests or personal relationships that could have appeared to influence the work reported in this paper.

Acknowledgments

References

[1] Z. Feng, J. Ling, M. Ming, W. Liang, K.K. Tan, X. Xiao, Signal-transformation-based repetitive control of spiral trajectory for piezoelectric nanopositioning stages, IEEE/ASME Trans. Mechatron. (2020).
[2] D.-S. Sohn, Clinical utilization of ultrasonic piezoelectric bone surgery during osteotomy, J. Korean Assoc. Oral. Maxillofac. Surg. 45 (4) (2019) 173.
[3] U. Bhattarai, A.T. Alouani, Flexible semi-automatic arm design for minimally invasive surgery, in: Proceedings of the 25th International Conference on Systems Engineering (ICSEng), IEEE, 2017, pp. 207–211.
[4] J. Ling, M. Rakotondrabe, Z. Feng, M. Ming, X. Xiao, A robust resonant controller for high-speed scanning of nanopositioners: design and implementation, IEEE Trans. Control Syst. Technol. 28 (3) (2019) 1116–1123.
[5] Z. Qiu, W. Piyawattanametha, Mems actuators for optical microendoscopy, Micromachines (Basel) 10 (2) (2019) 85.
[6] M. Silvestri, M. Confalonieri, A. Ferrario, Piezoelectric actuators for micro positioning stages in automated machines: experimental characterization of open loop implementations, FME Trans. 45 (3) (2017) 331–338.

[7] J. Ling, Z. Feng, M. Ming, X. Xiao, Damping controller design for nanopositioners: a hybrid reference model matching and virtual reference feedback tuning approach, Int. J. Precis. Eng. Manuf. 19 (1) (2018) 13–22.

[8] T. Ye, J. Ling, X. Kang, Z. Feng, X. Xiao, A novel two-stage constant force compliant microgripper, J. Mech. Des. 143 (5) (2020).

[9] R. Staehr, S. Bluemel, P. Jaeschke, O. Suttmann, S. Kaierle, L. Overmeyer, J.-P. Negel, C. Stolzenburg, Advanced macro drilling of carbon fibre reinforced plastics for aerospace applications, in: High-Power Laser Materials Processing: Applications, Diagnostics, and Systems VIII, 10911, International Society for Optics and Photonics, 2019, p. 109110N.

[10] S. Cardarelli, N. Calabretta, R. Stabile, K. Williams, X. Luo, J. Mink, Wide-range 2d INP chip-to-fiber alignment through bimorph piezoelectric actuators, in: Proceedings of the IEEE 68th Electronic Components and Technology Conference (ECTC), IEEE, 2018, pp. 1124–1129.

[11] J. Ling, Z. Feng, D. Zheng, J. Yang, H. Yu, X. Xiao, Robust adaptive motion tracking of piezoelectric actuated stages using online neural-network-based sliding mode control, Mechanical Systems and Signal Processing 150 107235.

[12] S. Wang, W. Rong, L. Wang, Z. Pei, L. Sun, Design, analysis and experimental performance of a novel stick-slip type piezoelectric rotary actuator based on variable force couple driving, Smart Mater. Struct. 26 (5) (2017) 055005.

[13] Y. Zhang, Y. Peng, Z. Sun, H. Yu, A novel stick–slip piezoelectric actuator based on a triangular compliant driving mechanism, IEEE Trans. Ind. Electron. 66 (7) (2018) 5374–5382.

[14] Z. Guo, Y. Tian, D. Zhang, T. Wang, M. Wu, A novel stick-slip based linear actuator using bi-directional motion of micropositioner, Mech. Syst. Signal Process. 128 (2019) 37–49.

[15] R. Wang, Y. Hu, D. Shen, J. Ma, J. Li, J. Wen, A novel piezoelectric inchworm actuator driven by one channel dc signal, IEEE Trans. Ind. Electron. (2020).

[16] S. Song, S. Shao, M. Xu, Y. Shao, Z. Tian, B. Feng, Piezoelectric inchworm rotary actuator with high driving torque and self-locking ability, Sens. Actuat. A 282 (2018) 174–182.

[17] W. Chen, Y. Liu, Y. Liu, X. Tian, X. Shan, L. Wang, Design and experimental evaluation of a novel stepping linear piezoelectric actuator, Sens. Actuat. A 276 (2018) 259–266.

[18] S. Mohith, P.N. Karanth, S. Kulkarni, Experimental investigation on performance of disposable micropump with retrofit piezo stack actuator for biomedical application, Microsyst. Technol. 25 (12) (2019) 4741–4752.

[19] Y. Liu, S. Shi, C. Li, W. Chen, L. Wang, J. Liu, Development of a bi-directional standing wave linear piezoelectric actuator with four driving feet, Ultrasonics 84 (2018) 81–86.

[20] J. Deng, Y. Liu, C. Weishan, L. Junkao, Development and experiment evaluation of an inertial piezoelectric actuator using bending-bending hybrid modes, Sens. Actuat. A 275 (2018) 11–18.

[21] Y. Zhang, M. Wang, Y. Cheng, D. Zheng, Y. Peng, A stick-slip/inchworm hybrid rotary piezo motor based on a symmetric triangular driving mechanism, Appl Phys Lett 115 (13) (2019) 131904.

[22] P. Pan, F. Yang, Z. Wang, B. Zhong, L. Sun, C. Ru, A review of stick-slip nanopositioning actuators, in: Nanopositioning Technologies, Springer, 2016, pp. 1–32.

[23] A.J. Fleming, S.S. Aphale, S.R. Moheimani, A new method for robust damping and tracking control of scanning probe microscope positioning stages, IEEE Trans. Nanotechnol. 9 (4) (2009) 438–448.

[24] J. Wang, Q. Lu, How are the behaviors of piezoelectric inertial sliders interpreted? Rev. Sci. Instrum. 83 (9) (2012) 093701.

[25] J. Tang, H. Fan, J. Liu, H. Huang, Suppressing the backward motion of a stick–slip piezoelectric actuator by means of the sequential control method (SCM), Mech. Syst. Signal Process. 143 (2020) 106855.

[26] F. Qin, H. Huang, J. Wang, L. Tian, T. Liang, H. Zhao, Design and stepping characteristics of novel stick–slip piezo-driven linear actuator, Smart Mater. Struct. 28 (7) (2019) 075026.

[27] J. Yao, J. Cai, Y. Hu, J. Wen, N. Wan, H. Wang, J. Li, An umbrella-shaped linear piezoelectric actuator based on stick-slip motion principle, IEEE Access 7 (2019) 157724–157729.

[28] X. Lu, Q. Gao, Y. Li, Y. Yu, X. Zhang, G. Qiao, T. Cheng, A linear piezoelectric stick-slip actuator via triangular displacement amplification mechanism, IEEE Access 8 (2020) 6515–6522.

[29] J. Li, H. Huang, H. Zhao, A piezoelectric-driven linear actuator by means of coupling motion, IEEE Trans. Ind. Electron. 65 (3) (2017) 2458–2466.

[30] J. Li, X. Zhou, H. Zhao, M. Shao, P. Hou, X. Xu, Design and experimental performances of a piezoelectric linear actuator by means of lateral motion, Smart Mater. Struct. 24 (6) (2015) 065007.

[31] Y. Zhang, M. Wang, Y. Fan, T.-F. Lu, Y. Cheng, Y. Peng, Improving load capacity of stick-slip actuators in both driving directions via a shared driving foot, Smart Mater. Struct. 28 (6) (2019) 065004.

[32] T. Cheng, M. He, H. Li, X. Lu, H. Zhao, H. Gao, A novel trapezoid-type stick–slip piezoelectric linear actuator using right circular flexure hinge mechanism, IEEE Trans. Ind. Electron. 64 (7) (2017) 5545–5552.